

Optimal Sensor Placement Strategy for Event Monitoring in Smart Homes

Khaled Mohammed^{1,2}

⁽¹⁾ Programming Technology Department, Sana'a Community College, Yemen

⁽²⁾ Administration Information System Department, Faculty of Economic &
Administration Science, Queen Arwa University, Yemen,
Khaled.Mohammed@scc.edu.ye

Abstract

Optimal sensor placement in smart homes aims at complete coverage, cost reduction and minimization of energy consumption. This paper presents a heuristic strategy for sensor placement through cooperation of multiple sensors. Wireless cams, passive infrared sensors (PIRs) and RFIDs cooperate through a master gateway. Algorithms are presented for the cooperative control of the smart home environment. First time using Minimum Ratio (MR) algorithm in smart home. System performance is evaluated through intensive use in a real home setting. Results indicated complete coverage of home areas, optimal number of sensors and high savings in both energy consumption and video-storage requirements.

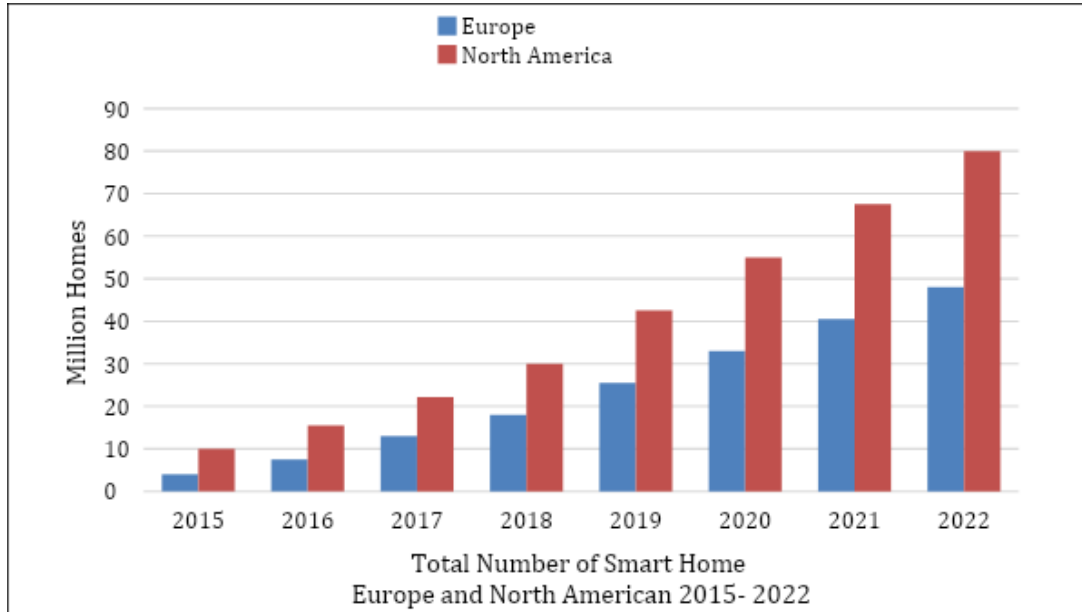
Keywords: SMEs, integrated systems, risk management, information security, business continuity, Internet of things, smart homes, optimal sensor placement, Minimum Ratio, and cooperative control..

1. Introduction

It has been predicted that a typical home could be equipped by more than 500 smart devices by 2022 [Gartner]. These smart devices will raise the standard of the quality of living by helping inhabitants to seamlessly control their homes and make smart decisions. Smart devices and related applications collect data which aims at automation of most activities in family homes. The key drivers for adopting smart homes are: personal and family security, health monitoring, efficiency of energy consumption, convenience in programming home settings and maintenance, higher productivity and ability to manage work-life balance, easier network access and information sharing with others, faster home delivery and better entertainment [1]. Self-learning smart devices are the consumers' ultimate goal. On the other hand, the major concerns related to smart device adoption are privacy/data concerns and interoperability concerns [1]. In [2], Energy management and climate control systems, Security and access control systems, Lighting and window control systems, Home appliances, Healthcare and assisted living Multifunction and whole-home automation systems and Audio-visual and entertainment systems are considered the major drivers

for smart home adoption and it has been predicted that 148 million homes in Europe and North America will be smart by 2023 (Figure 1).

Figure 1
Predicted growth of smart home adoption [2]



Ensuring both the comfort ability and safety of smart home inhabitants it is essential to optimize the placement of sensors in a smart home in order to improve the system performance and minimize its cost. This paper presents a heuristic approach for sensor placement. The rest of the paper is organized as follows. Section 2 overviews the related work. Section 3 presents the heuristic sensor placement strategy. Section 4 describes the cooperative sensing system. Section 5 describes the system architecture, whereas Section 6 provides some implementation details. Section 7 presents the experimental results. Finally, Section 8 concludes the paper.

2. Related Work

There are many approaches in the literature for optimizing sensor placement smart homes such as: Human intuition-based placement [3], Hill Climbing [4], Probabilistic Models [5-6], Sub modular Optimization [7-8] and Genetic Algorithms. The generated placements are evaluated based best coverage, minimum number of sensors, minimum cost and minimum energy consumption. Selection of sensor type greatly affects the sensing cost. Good placement strategies help minimize sensor number and maximize its coverage area. In this research, a suitable optimization technique is presented, tested and its effectiveness is evaluated in a real smart home setting. Brian et al. [4] proposed five different approaches to sensor placement are

evaluated and compared for future use. It has been concluded that sensor placement based of Genetic Algorithm Optimization has resulted in the best results. Activity recognition accuracies for the different approaches are summarized in the following Table 1 [4]:

Table 1

Comparison between different sensor placement approaches [4].

Placement Approach	Recognition Accuracy	Standard deviation
Human intuition	76.01%	2.36
Monte Carlo	75.71%	8.48
Grid 10x10	93.54%	0.28
Hill climbing	96.44%	1.64
Genetic Algorithm	97.17%	1.33

Fanti et al. [9] proposed Integer Linear Programming based optimization has been applied for sensor placement in smart homes in order to track inhabitant's locations using motion detectors. Minimum sensors cost and maximum coverage were the objectives of the optimization process on a 2D grid. Khan and Shah [10] proposed Wireless Camera Network Control (CWCNC), many strategies for allocation and scheduling of cameras to track objects and recognize them. In [10], consistently labeled objects are tracked using a camera network with cameras having overlapping FOVs. A second strategy is to link the active cameras and use location and direction of motion for allocation of the camera which should take over the observer task. In this paper, the linkage between cameras is achieved through a set of PIRs to adaptively locate the moving target and accordingly to direct the camera towards it as an object of interest. Some problems such as multiple persons moving at home in different places and together at the same or different times impose a heavy burden on the camera network collaboration and coordination strategy. Some research has been conducted to solve some of the uncertainties associated with dynamic scenes [11-15]. Essa et al. [16] proposed a Minimum Ratio (MR) for defect detection system The system is based on scanning the input image by a sliding window that is divided into a number of cells and then computing minimum ratio from eight neighboring cells to the current examined one. The final decision is reached by using ELM classifier to determine whether the window has a defect or not. The accuracy of defect detection is 98.07%. Mohammed et al. [17] presents an effective solution for the real-time student attendance management problem in large lecture halls. Fast response time and high accuracy imply using high-speed technologies and processes for student identification. Radio Frequency Identification (RFID) and novel face recognition and identification approaches have been proposed and evaluated. A multimodal approach

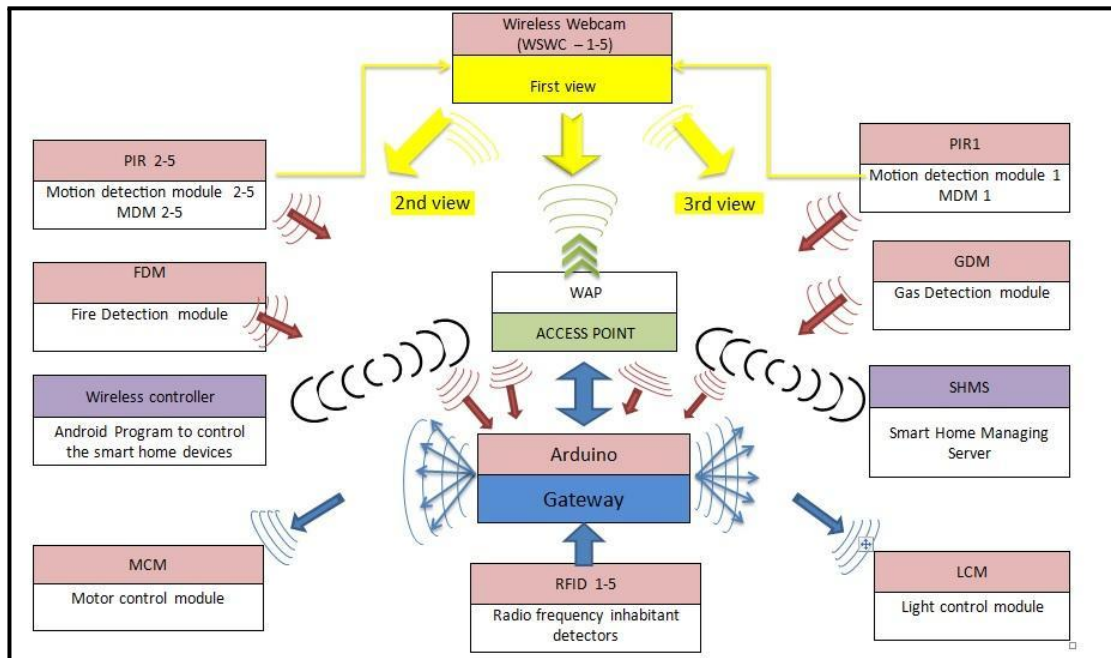
for student identification combined the power of both the traditional RFID approach and Multi-Scale Structural Similarity (MS-SSIM) index. Capturing the authentic face variability from a sequence of video frames has been considered for the recognition of faces and resulted in system robustness against the variability of facial features. It achieved an accuracy of 99%. Raafat at al. [18] proposed new a new approach for novelty detection in sensor signals based on Levene’s test which tests the homogeneity of variances of samples taken from the same population and combined with other statistical and autocorrelation features. The authors used MR technique for Statistical feature extraction which reflects the similarity of two successive sensor signal windows X1 and X2, the accuracy reached 98.44% while both sensitivity and precision reached 96.49% and 100.00%.

3. System Architecture

A smart home management system (SHMS) consists of a main control gateway which wirelessly communicates with a smart set of wireless sensor modules (WWC, MDM, FDM, GDM, MCM, LCM and RFIDs). Figure 2 shows the relationship between the different system components.

Figure 2

Smart Home System.



3.1 Gateway

A gateway (Figure 3) acts as an anchor device which controls the activation of the wire-less webcams adaptively according to the activities of smart home inhabitants. For ex-ample, the first webcam (WC) located at the entrance hall starts recording the activity of an entering inhabitant. Once the inhabitant disappears from the FOV of the

WC, the gateway (Anchor device - with wireless connectivity) initiates a second WC based on a PIR signal received from the new inhabitant location which lies outside the coverage area of the first Wireless Camera.

Figure 3
 Gateway Microcontroller.

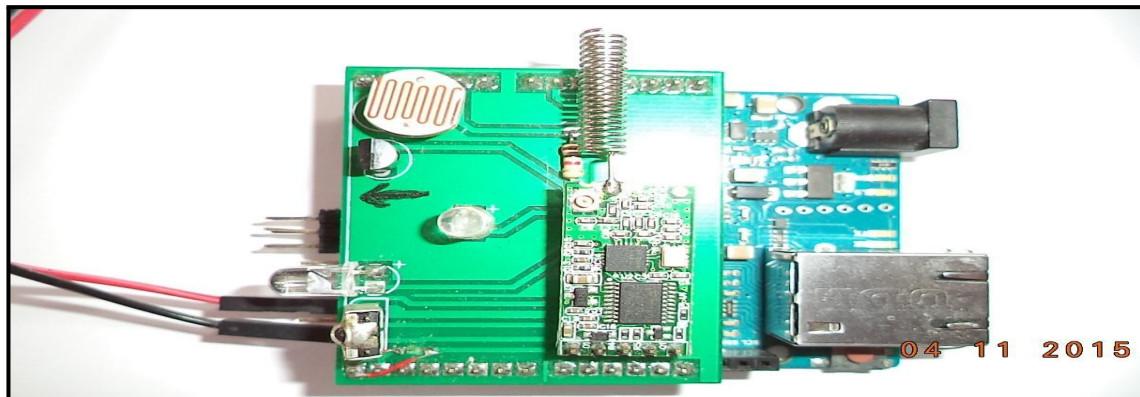


Figure 4
 Gateway Microcontroller.

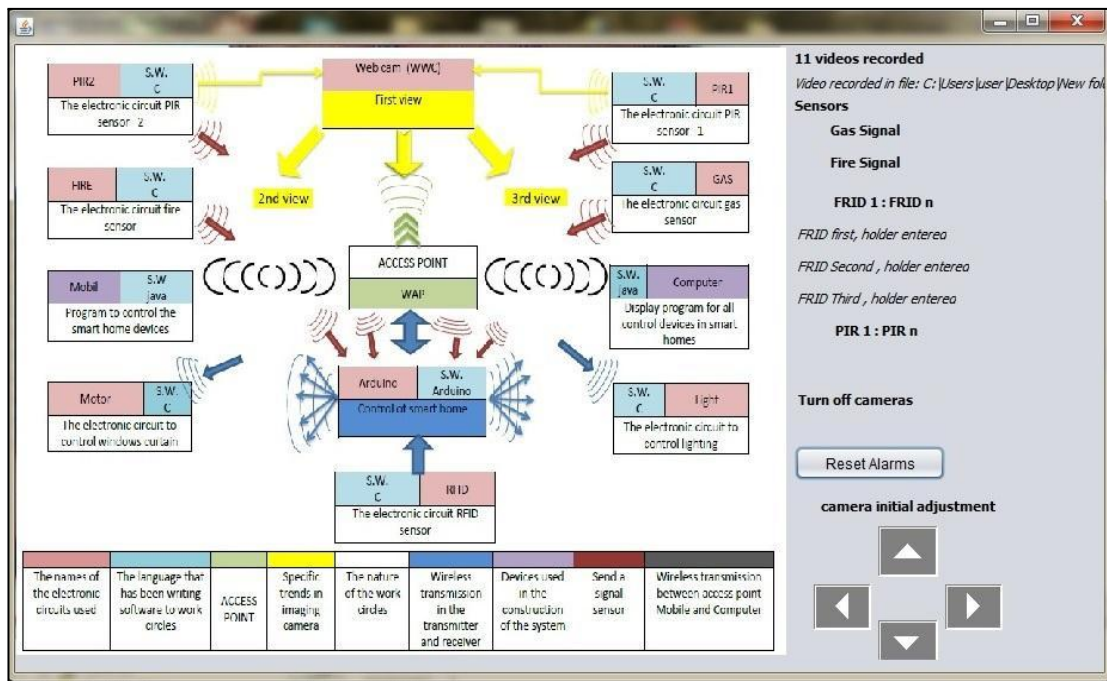


Figure 4 Shows the GUI for the gateway which controls all the smart home operations.

3.2. Sensing/Actuation Layer

The smart home is equipped with a large set of sensors which are used to detect motion (PIRs, Wireless web cams, light), presence/absence, and moisture metering sensors, temperature sensors, light sensors, gas sensors, smoke sensors, and RFID devices. Curtain actuators are also used. Sensors are classified into master sensors and slave sensors. A PIR which detects a moving target acts as a master sensor. A wireless webcam which starts tracking the detected moving target is a slave sensor. RFID reader which reads a personal tag serves as an authenticator of the personality of the inhabitant whose video is recorded by a second WWC.

3.4.1. Curtain Control Module (CCM)

Figure 5

Curtain Control Module (Cont.).

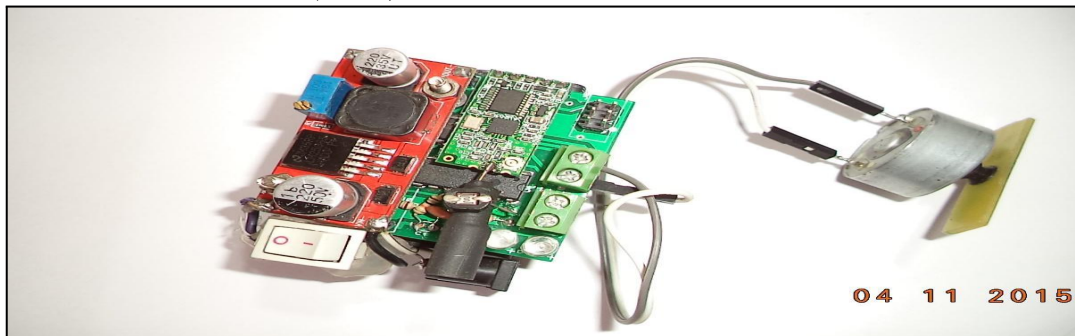


Figure 5 shows the Curtain Control Module (Cont.). The motor control circuit will control the speed of two connected DC motors as well as control the speed. The motor circuit receives the signal and executes the commands “open and close the curtains.

3.4.2. Motion Detection Module (MDM)

Figure 6

Motion Detection Modules.

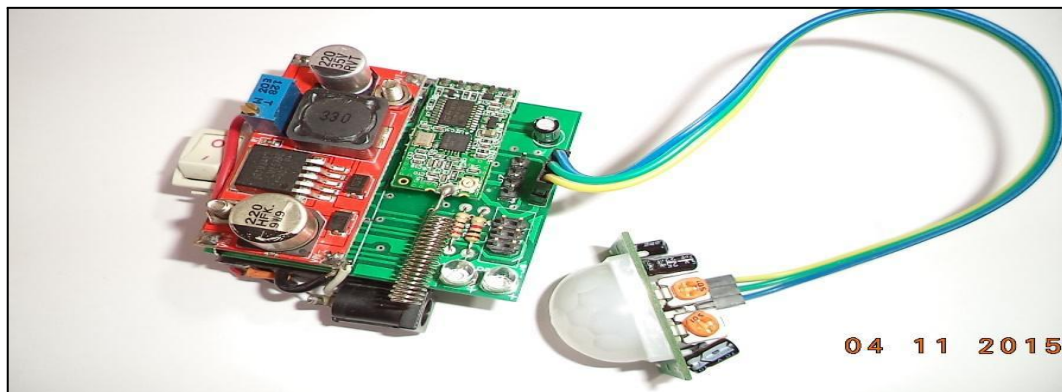


Figure 6 shows the MDMs distribution in an experimental home. MDMs are placed in all places where inhabitants frequently move. PIR data is wirelessly transmitted from MDM to the Arduino based gateway through a wireless access point. Figure 8 shows the Smart Home Server (SHS). The sensory data received from sensors are processed for decision making. Detected motion initiates the wireless camera for video event detection to save storage and processing cost. Motion detectors in smart home could be classified into three types:

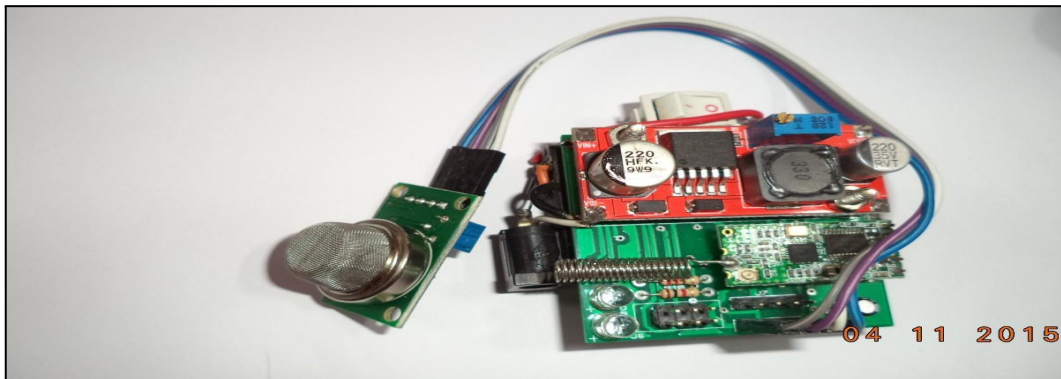
- (1) Wireless cameras
- (2) Passive Infra-red (PIR) detectors
- (3) Light sensors

The PIR motion detection module is shown in Figure 6. The module includes the binary mode PIR sensor, a wireless communication module and a control board based on ATME88, microcontroller. The module is powered by a chargeable battery. The MDMs are allocated at important entries in the smart home like the doors of home, rooms, kitchen and bath room.

3.4.3. Gas/Fire Sensing Module (GFSM)

Figure 7

Gas/Fire Sensing Module (GFSM).



In figure 7, an Analog gas/smoke sensor (MQ-2) is used for both smoke and gas leakage detection the kitchen. MQ-2 is sensitive to the liquefied Petroleum Gas (LPG), i-butane, propane, methane, alcohol, Hydrogen and smoke [19]. Data acquisition is controlled by an Atmiga Microprocessor. It communicates through WiFi with the Gateway. The control module issues an alarm and informs the Gateway of fire/gas leakage which subsequently which could initiates a phone call.

3.4.4. Light Control Module (LCM)

Smart lighting control module saves energy, increases convenience, through light on/off switching, and dimming and is used for active motion detection for home security. Light control is either initiated by the inhabitant through an android

application on the smart phone of through recognition of the inhabitant activities. Figures (8-9), show the SML control module which is provided with WiFi, and solar energy power supply which stores energy during night lighting the home. And the light dimmer circuit design has been improved to utilize the power consumption. The module has the advantage of solar energy collection for modules battery charging.

Figure 8
Light Control Module (LCM)

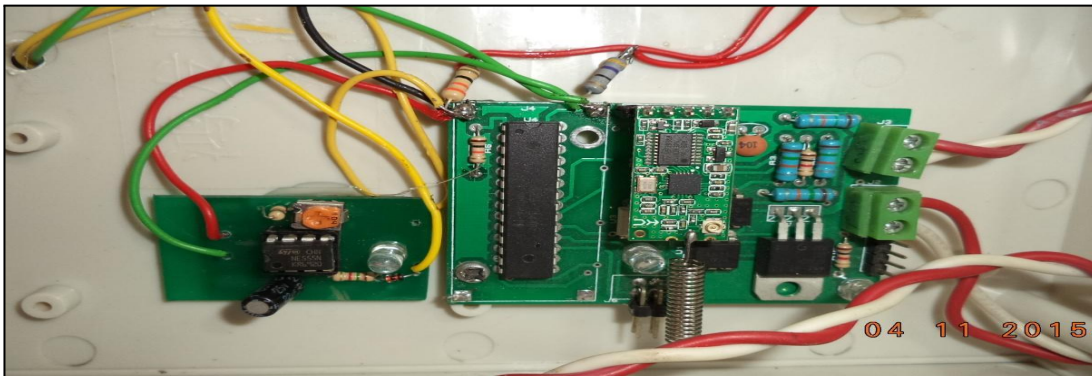


Figure 9
Light Control Module (LCM) - Solar Energy



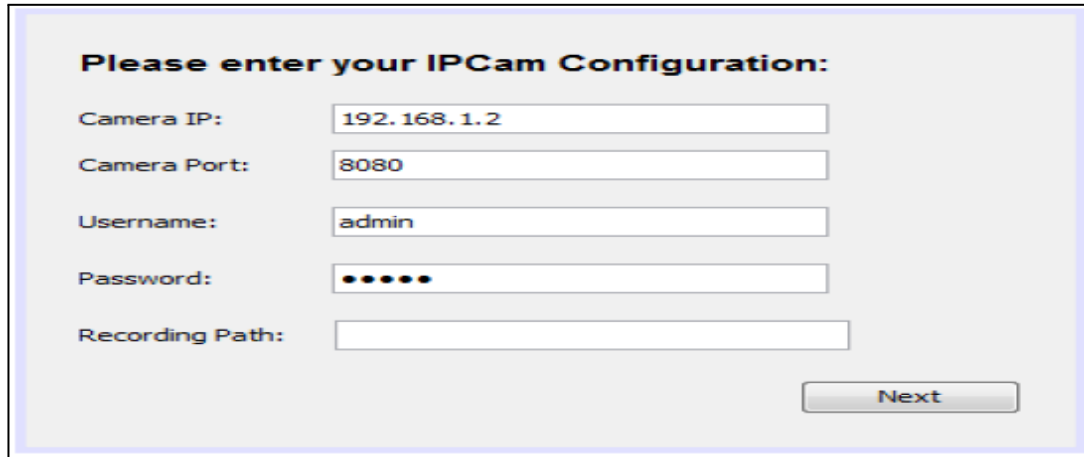
It is appropriate to declare confidently through the risk management, there is congruence with ISO 27001 (information security), ISO 22301 (business continuity), cybersecurity and, consequently, the information technologies, being a key point for the integration based on similarity and standardization criteria's, and as a result from the analysis performed for the methodologies related with the researching, it is

concluded that the PDCA methodology is a holistic approach and is keeps consistent relationship with factors established in the integration. As shown in Figure 4.

3.4.5. Wireless Camera Control Module (WCCM)

Figure 10

GUI Interface of the WCCM



The image shows a web-based configuration form for an IP camera. The title is "Please enter your IPCam Configuration:". Below the title are five input fields: "Camera IP:" containing "192.168.1.2", "Camera Port:" containing "8080", "Username:" containing "admin", "Password:" containing five dots, and "Recording Path:" which is empty. A "Next" button is positioned at the bottom right of the form.

Figure 10 shows the GUI for the configuration of the Wireless Camera Control Module (WCCM). Collaborative Wireless Camera Network Control (CWCNC) is presented as a means for optimal visual sensor localization tool in smart homes. This approach helps minimize system cost, optimize coverage area and saves a lot of energy and storage area. Monitoring of a smart home environment requires an optimally allocated set of wireless cameras and a smart collaboration approach to accurately track motion and activate sensors and actuators according to serve the Smart Home Inhabitants (SHIs). To optimally allocate the cameras in a SH, system design has to avoid the constraints imposed by both moving object occlusion and walls. The Field Of View (FOV) of each camera plays a crucial role in system design. Other factors which have impact on sensor (camera) localization, are the rotation, tilt and zooming. Smart algorithms have to consider all these factors to accurately detect motion, recognize events and actuate things.

This paper presents a new algorithm for collaborative camera control (CCC or C3) which solve the following problems:

- (1) Camera calibration
- (2) Rotation, tilt, zoom and FOV
- (3) Occlusion and obstacle avoidance
- (4) Focusing on the Object Of Interest (OOI)
- (5) Context awareness (Inhabitant' behavior and SH content)
- (6) Energy consumption (Smart power management – Energy Harvesting)
- (7) High cameras cost

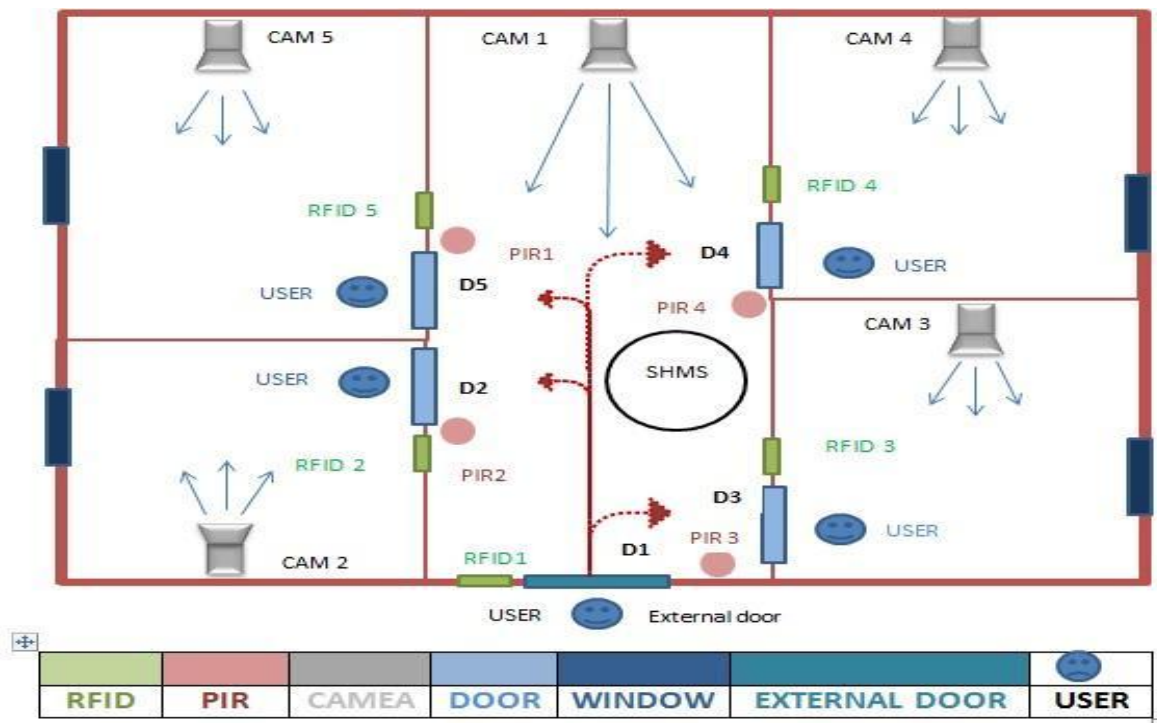
- (8) Massive video storage requirements
- (9) Costly video processing (context triggered processing)

4. Sensor Placement Strategy

Figure 11 shows the arrangement of sensors in a smart home. Sensors are located according to the activity level of the Smart Home Inhabitants (SHIs). To optimize sensor allocation, many factors are considered such as:

- (1) Inhabitants activity frequency
- (2) Maximum network coverage area
- (3) Minimum energy consumption
- (4) Minimum sensor cost
- (5) Sensor type
- (6) Maximum communication reliability.

Figure 11
Sensor placement in smart home



Floor Plan in a Smart Home.

5. Algorithms of the Smart Home Management System (SHMS)

The smart home intelligent gateway implements many different intelligent algorithms 5.1 -5.3 for motion detection, one of them algorithms (MR) uses the first time in Face Recognition, novelty detection (light change, gas leakage, smoke, etc.) and management of energy consumption and harvesting:.

Algorithm 5.1: Tracking and identifying the movement of persons in Smart Home

Input: Initialize the devices “cameras, PIR Sensors, RFID Sensors” and set the center of view for the cameras

Output: Starting Record Video

1. For i=1 to N do
2. Calculate the MR values for each two successive frames for 100 times
3. Calculate both the mean and standard deviation of the 100 MR values according to the following formulas
4. Get the threshold limit for motion detection based on MR Value:

$$\theta = \mu \pm 3\sigma \quad (1)$$

$$\mu = \frac{\sum_{i=1}^{100} \theta_i}{100} \quad (2)$$

$$\sigma = \sqrt{\frac{\sum_{i=1}^{100} (\theta_i - \mu)^2}{100 - 1}} \quad (3)$$

5. IF a motion is detected in Main Camera then
6. Start video recording until motion stops
7. End IF;
8. IF a PIR sensor detects motion at a certain door then
9. Redirect the camera to towards that door
10. Start recording until the moving person disappears from the camera viewing area
11. End IF;
12. Check the RFID reading with the records in Data set
13. IF the RFID Tag has found the record in the dataset OR the PIR has not discovered the move-ment during a specified time then
14. Stop recorder in this camera and run the main camera.
15. End IF;
16. IF the RFID Tag is not in dataset then

17. The camera starts recording.
 18. End IF;
 19. End For;
-

Algorithm 5 2: Tracking and identifying the movement of persons in Smart Home

Input: Initialize all devices: PIR Sensors, Gas Sensors, Fire Sensors, Cameras, RFID Sensors, Motors and Light Sensors” and set the center for cameras views.

Output: Services and protection in Smart Home

1. Foreach Circuit gets the IP’s of the main microcontroller
 2. Connect with the Mobile or server using the access point Wi-Fi.
 3. IF the fire sensor detects a fire in the home then
 4. Fire sensor sends a signal to the microcontroller for reporting the presence of fire.
 5. Server sends a sound warning and a mobile message.
 6. End IF;
 7. IF the gas sensor detects gas leakage in the kitchen or bathroom then
 8. Gas sensor sends a signal to the microcontroller for reporting the presence of gas.
 9. Server sends a sound warning and a mobile message.
 10. End IF;
 11. End Foreach;
 12. Foreach person at home using the light service during smart home application in mobile
 13. the mobile sends a signal to the light circuit through the microcontroller
 14. IF light circuit gets any signal from mobile then
 15. Light circuit receives the signal
 16. Executes one of the commands “Reduce and increment the light at home, close and open the light”.
 17. End IF;
 18. End Foreach;
 19. Foreach person at home using the Motor service through smart home application in mobile
 20. IF the motor circuit gets any signal from mobile then
 21. The motor circuit receives the signal
 22. Executes one of the commands “open and close the curtains, Fumbles the presence of light, open or close the doors”
 23. End IF;
 24. End Foreach;
-

Algorithm 5.3: Smart Energy Harvesting in a SHE (Smart Home Environment)

1. Use solar energy collectors to collect energy from Electric Lamps during the night time where the electric system is lighting the home.
 2. Cameras and PIRs are powered with solar cells which are energized by the SHLES (Smart Home Electric Lighting System)
 3. Monitor the charging level of the batteries of Wcams and PIRs
 4. Switch on the Solar Energy Collectors to activate charging
-

6. De-noising of Sensor Signal

Complete Ensemble Empirical Mode Decomposition (CEEMD) [20] is one of the most recent techniques for signal de-noising. The sensor signal $x(t)$ is first decomposed into its Intrinsic Mode Functions (IMFs) (Figure 16). The filtered signal $y(t)$ is reconstructed by discarding the first IMF and construction the filtered signal according to the following formula:

$$y(t) = \sum_{i=2}^N IMF(i) \quad (4)$$

Where N is the number of the IMFs. It has been implement here for removing the high frequency noise of most sensor signals. Figure 12 show the light signal acquired by an LDR and its filtered version using the CEEMD. It could be seen that the high frequencies are filtered out and the important light signal features are preserved.

Figure 12

LDR Signal (top) and de-noised signal (bottom) using CEEMD

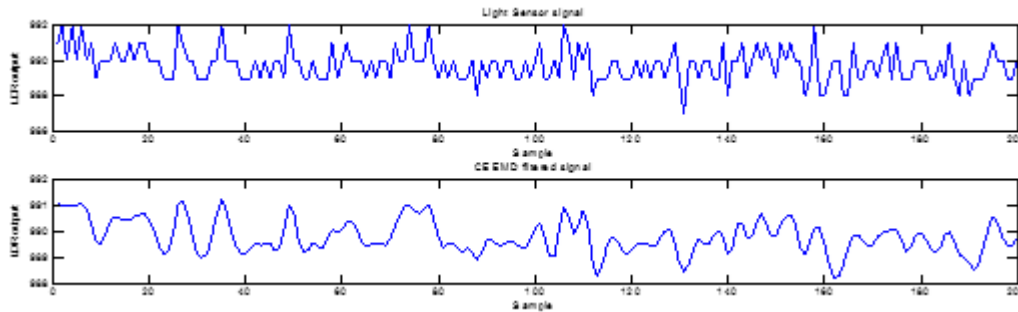
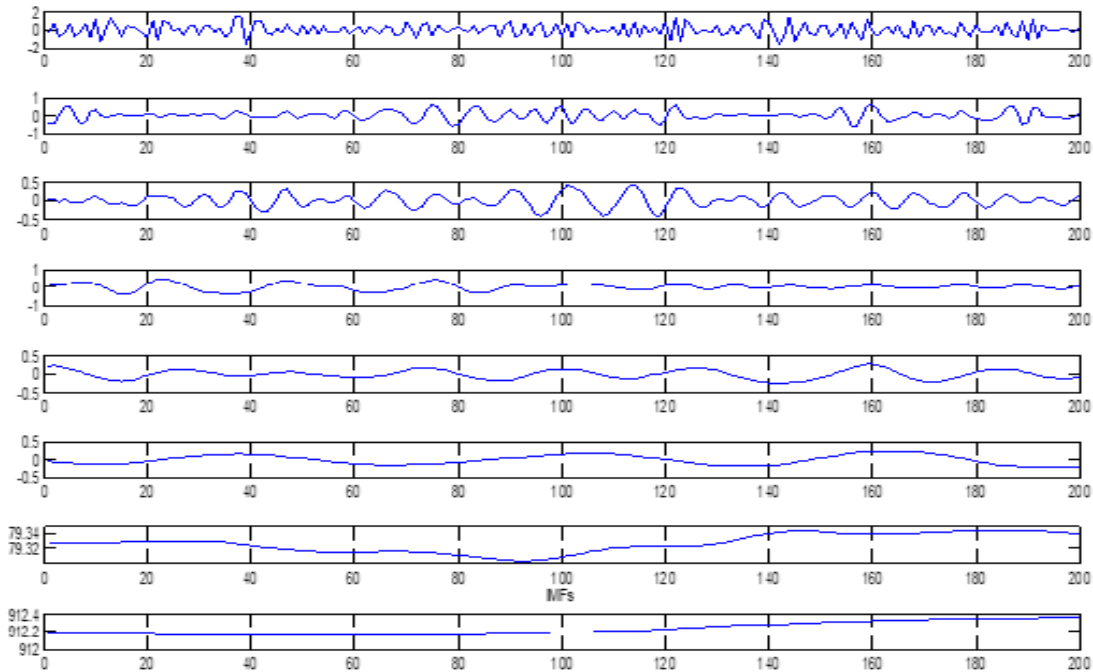


Figure 13 shows the intrinsic mode function of the LDR signal. It could be noticed that the high frequency noise is represented by the first IMF. According to the normative form of integration, there are various deliverables are related to the GIS:

Figure 13
Intrinsic Mode functions of the LDR signal



6.1. Feature Extraction for State Identification/Event Detection

To help tackle analyzing the deluge of data acquired by a huge set of sensors, efficient feature extraction techniques have to be developed. In this paper, real-time sensor signal is being filtered using the Complete Ensemble Empirical Mode Decomposition (CEEMD). Three different dispersion measures have been applied for novelty detection in sensor signals:

- (1) Minimum Ratio (MR)
- (2) Auto correlation function.
- (3) Skewness, kurtosis and sum of the ACF from the ACF.
- (4) Pearson coefficient of correlation
- (5) Coefficient of variation(COV)
- (6) Moment of inertia (MOI)

6.1.1 MR AND MR based motion detection

In [21], the authors presented the details of the Multi Scale Structure Similarity Measurement System (MS-SSMS) and its application for motion detection in a smart home setting. For more details, the reader can refer to [21].

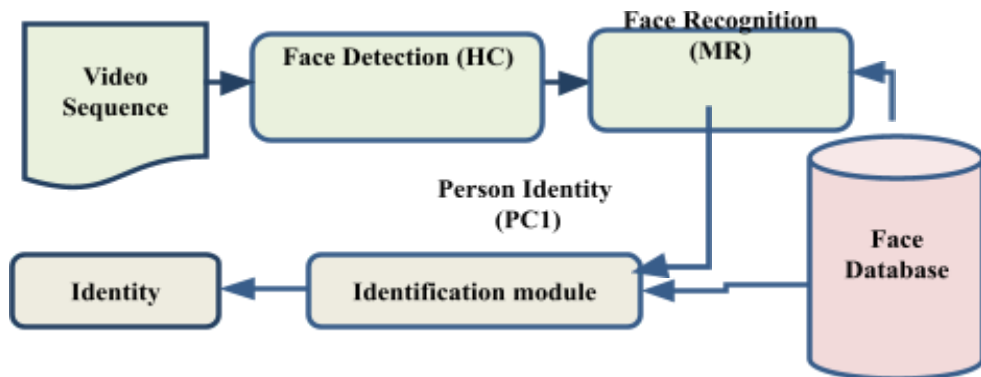
Our proposed system first time using MR Rules for motion detection between two images, original images (image1) which stored in motion database and sliding window (image2) that comes from the live camera, each image has the same dimension $n \times m$, each image has 24×24 pixels. The system is based on computing the minimum ratio between every two cells which have the same row and column in the images, the minimum ratio ω between two Images is calculated according to the following formula [16-18]:

$$\omega_{A,B} = \frac{1}{n*m} \sum_{i=1}^n \sum_{j=1}^m \min \left\{ \frac{A_{i,j}}{B_{i,j}}, \frac{B_{i,j}}{A_{i,j}} \right\} \quad (5)$$

where $A_{i,j}$ is cell in image1, $B_{i,j}$ is the same cell in image2, $\omega_{A,B}$ is a present value of MR between two images, If the two images look similar then the $\omega_{A,B}$ will be increased more than threshold, this paper presents the first application of the MR for motion detection in real-time, as shown in Figure 14. To ensure that the face to be recognized by the system is a live face, motion detection has also been implemented using MR. Figure 14 the multi-model person identification system based on HC, MR.

Figure 14

The multi-model person identification system based on HC, MR [17].



6.1.1.1 Adaptive Thresholding for Triggering Motion Recording

Estimation of the appropriate threshold level for the SSI test is very critical to the success of the presented motion detection system. The system is configured to work for a specific environment by adaptively calculating the motion detection threshold based on the difference between two successive frames. During the configuration phase, the average similarity index of N=100 pairs of two-successive frames is calculated together with the standard deviation. Then the similarity threshold is calculated according to the following equation:

$$\theta = \mu - 3\sigma \quad (6)$$

$$\mu = \frac{\sum_{i=1}^N \omega(A, B)}{N} \quad (7)$$

$$\sigma = \sqrt{\frac{\sum_{i=1}^N (\omega(A, B)_i - \mu)^2}{N - 1}} \quad (8)$$

During the implementation phase, if the similarity of two successive video frames is lower than θ , motion is detected and recording starts until the MR Value exceeds the threshold.

6.1.1.2 Enhanced Minimum ratio based Motion Detection Algorithm

MR has been used the first time for motion detection in videos and its performance has been evaluated. Evaluation results showed that the MR based method outperformed the well-known motion detection techniques. Motion detection accuracy ranges 99% in most experiments. The major advantages of the presented approach are: the higher motion detection accuracy and the fast processing speed. The problem which faces this method is the selection of the suitable threshold limit. In this paper, section 6 introduced an adaptive method for threshold selection. In [21], a fixed threshold level has been used for the MR based motion detection, which is very critical to the success of the presented detection system, in the same way Applies the rules in MR. The adaptive threshold selection presented in section 6 solves this problem. Figure 15 shows the layout of the combined module for face recognition using both Eigenfaces and MR

Algorithm 6.1: MR Based Motion Detection

Input: Two successive image frames f_t and f_{t+1}

Output: Motion or no-motion status

1. *Start video capture.*
 - i. *Calculate anadaptive MR threshold.*
 - ii. *Calculate the $\omega_{A,B}$ for every two successive frames for 10 Times.*
 - iii. *Calculate both the mean and standard deviation of the 10 MR values according to the following formulas to get the threshold limit for motion detection [25]:*

$$\theta = \mu - 3\sigma$$

$$\mu = \frac{\sum_{i=1}^N \omega(A, B)}{N}$$

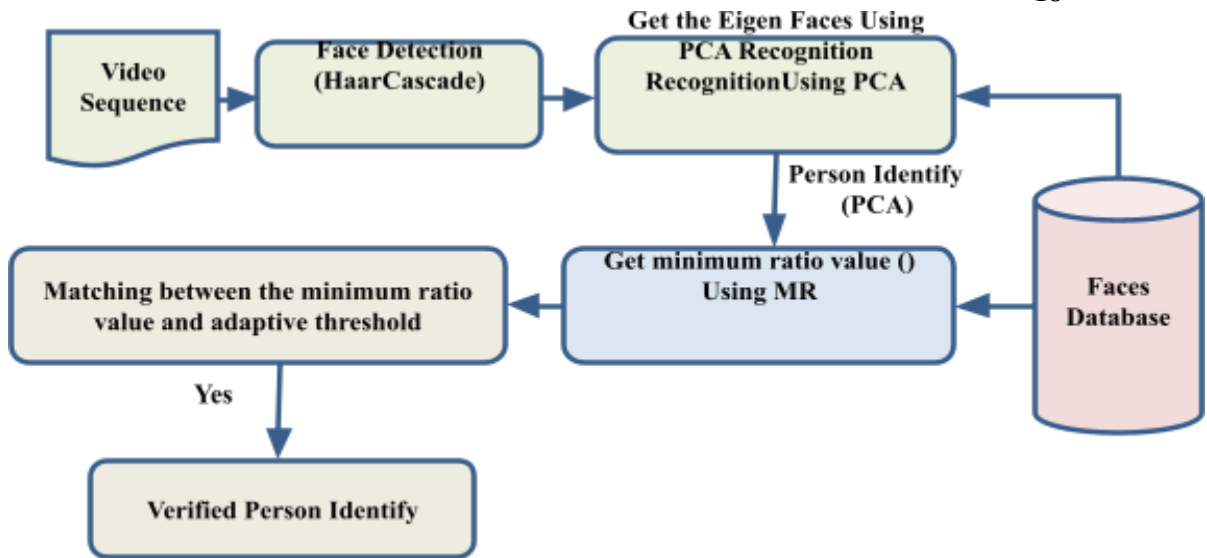
$$\sigma = \sqrt{\frac{\sum_{i=1}^N (\omega(A, B)_i - \mu)^2}{N - 1}}$$

2. *For $i=1$ to N Persons Do*
3. *Capture two successive frames f_t and f_{t+1} and Calculate $\omega_{A,B}$*

IF $\omega_{A,B} > \theta$ then
Status = live Person image
Else
Status = still Person image
End IF;
4. *End For;*

Figure 15

The layout of the combined module for face recognition using both Eigenfaces and MR.

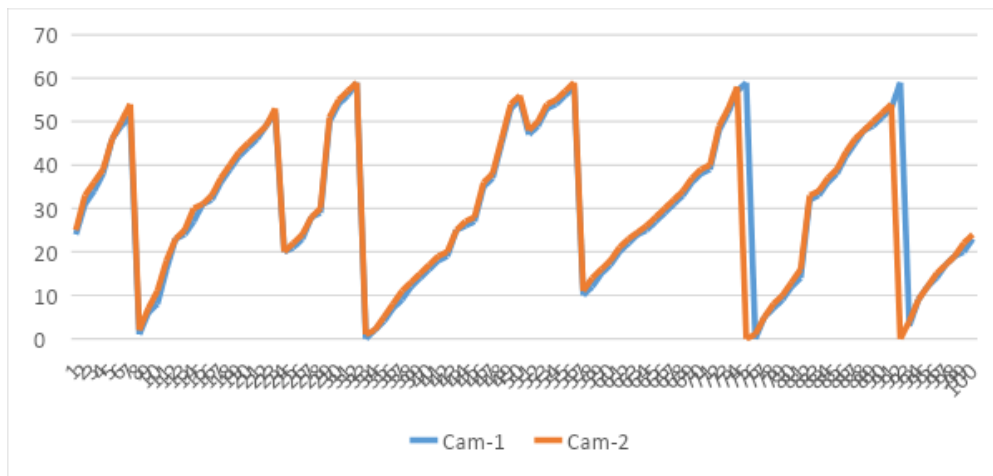


6.1.1.3 Event Triggered Camera Switching case

A case for switching between cameras based on the context has been evaluated based on a preplanned scenario. All switching cases were successful resulting in a sensor cooperation accuracy of 100%.

Figure 16

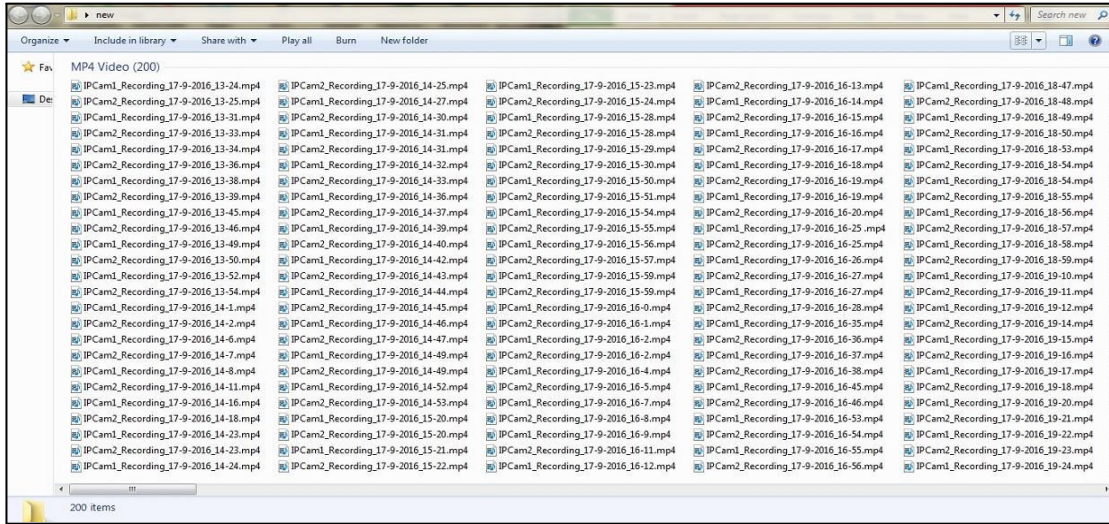
Switching times for WCAM1 and WCAM2.



Figures 16-17 shows the complete cooperation of the Wireless Cameras WCAM1 and WCAM2 in covering the events happening in two separate rooms based on forwarding control based on sensed motion by a PIR. Figure 18 shows the switching times and their succession through motion.

Figure 17

Switching times for WCAM1 and WCAM2.



6.1.2 Autocorrelation Function (ACF) based feature extraction

The Autocorrelation function $R(\tau)$ of the sensor signal $x(t)$ of N samples is calculated according to the following formula [20]:

$$R(\tau) = \frac{1}{N - \tau} \sum_{i=0}^{N-\tau-1} (x(i)x(i + \tau)) \quad (9)$$

Skewness, Kurtosis and the sum of the ACF values for 10 lags are calculated according to the following formulas:

$$Kurtosis = \frac{\mu^4}{\sigma^4} \quad (10)$$

Where, μ^4 is the fourth moment about the mean μ of the ACF values and σ is the standard deviation of the ACF.

$$Skewness = \frac{1}{N} \sum_{i=1}^N \left(\frac{x_i - \mu}{\sigma} \right)^3 \quad (11)$$

Where, N is the number of samples. The sum of the values of the ACF at different lags is also calculated as follows:

$$Sumacf = \sum_{\tau=1}^L R(L) \quad (12)$$

Where, L is the lag at which the ACF

Case Study 1: Soil Moisture in Smart Home Garden

To detect soil dryness in a moisture sensory signal (Figure 18), the de-noised signal is used to extract a highly discriminative feature set which includes the following features

Figure 18

Moisture sensor readings for wet soil.

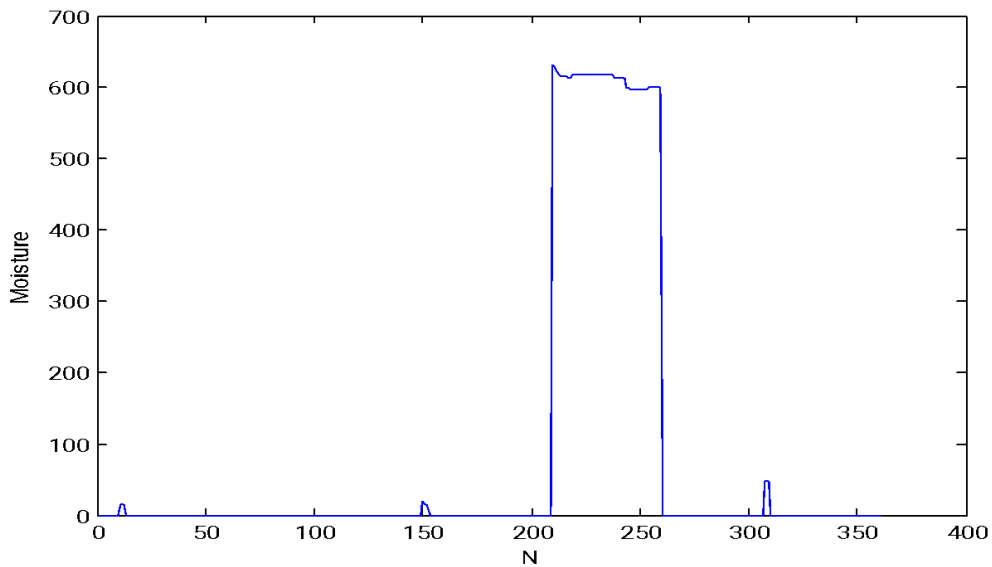


Figure 19

ACF of moisture sensor data for the case of wet soil.

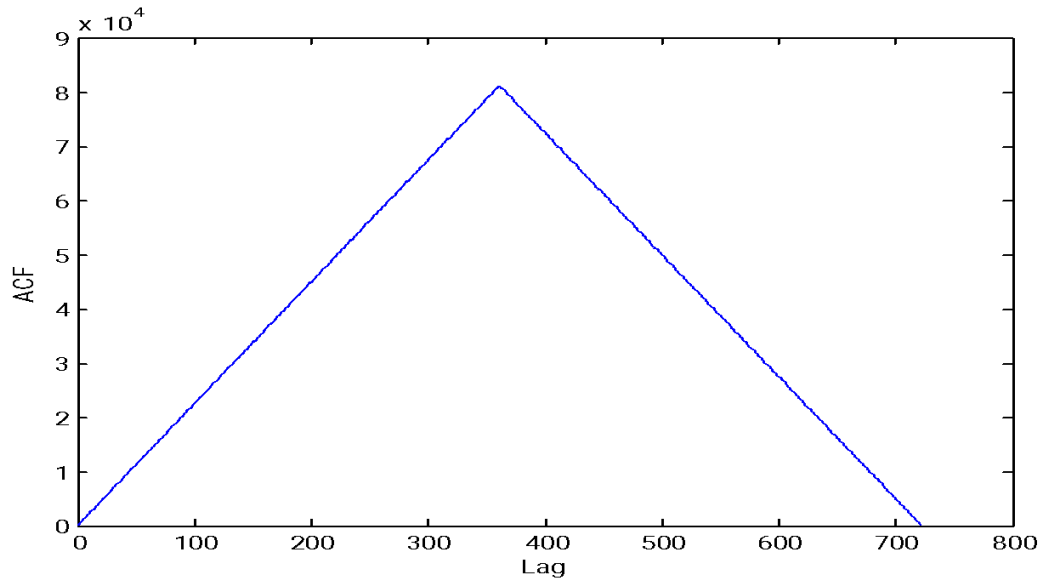
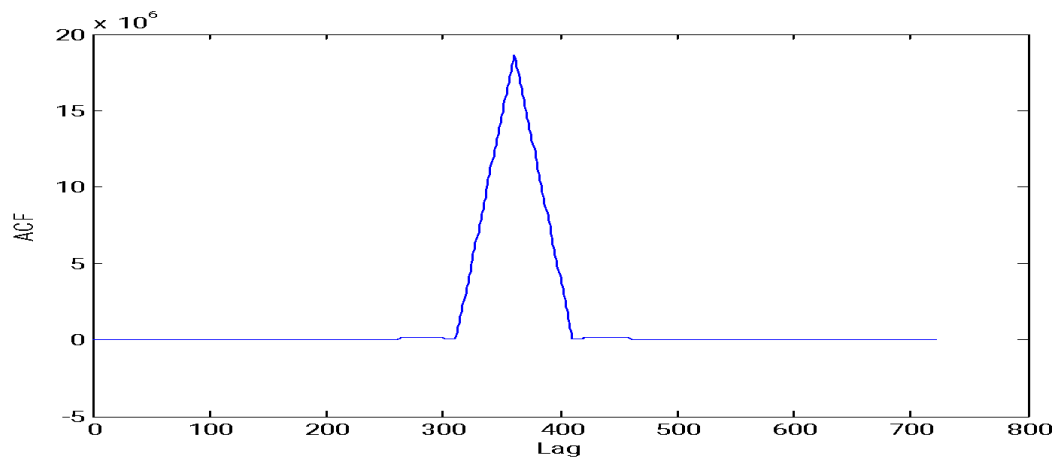


Figure 20
ACF of a dry soil sensor signal.



Figures 19 and 20 show the autocorrelation functions in the cases of wet soil and dry soil respectively. A change in moisture sensor signal is easily detected by extracting the following features: Skewness, Kurtosis and the sum of the ACF values for 10 lags. Table 2 gives the feature set values for both dry and wet soil cases. Both skewness and kurtosis result in small values in the case of wet soil and large values in the case of high wetness. The sum of the correlation coefficients for 10 lags increases with more wet soil.

Table 1
ACF based features extracted for wet and dry soil.

Feature/State	Dryness	Wetness
Skewness	2.1801	0.0396
Kurtosis	6.7777	1.8204
Sum of the ACF values for 10 lags	2.6154	18.7961

Case Study 2: Light change event detection

Figure 21

SumACF for 5 normal- and 5 abnormal cases.

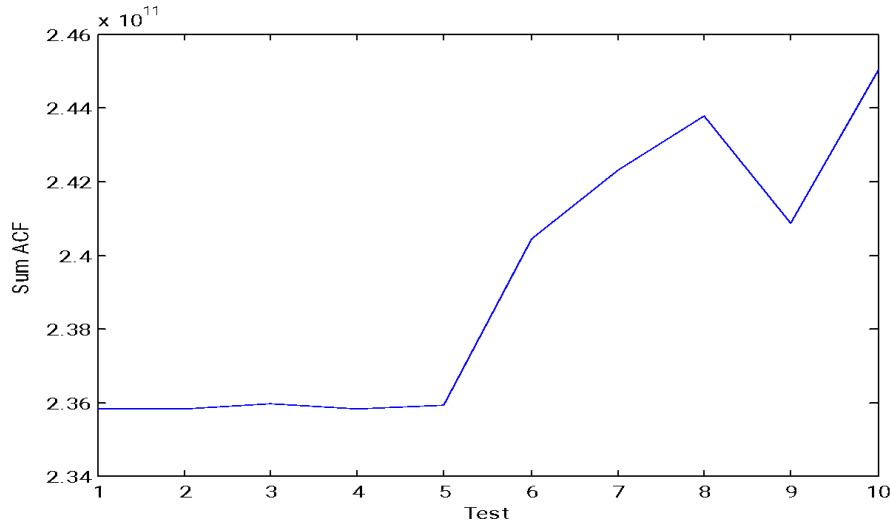


Figure 21 shows SumACF for 5 normal - and 5 abnormal cases. Abnormal light events result in increased ACF at different lags and consequently larger sum of the ACF values.

6.1.3 Pearson coefficient of correlation (r)

The correlation coefficient between sequences $x = \{x_i : i = 1, \dots, n\}$ and $y = \{y_i : i = 1, \dots, n\}$ is defined by [22]

$$r = \frac{\sum_{i=1}^n (x_i - \bar{x})(y_i - \bar{y})}{\sqrt{\sum_{i=1}^n (x_i - \bar{x})^2} \sqrt{\sum_{i=1}^n (y_i - \bar{y})^2}} \quad (13)$$

Where:

$$\bar{x} = \frac{1}{n} \sum_{i=1}^n x_i, \quad \bar{y} = \frac{1}{n} \sum_{i=1}^n y_i$$

Figure 22
 Moisture data – first window.

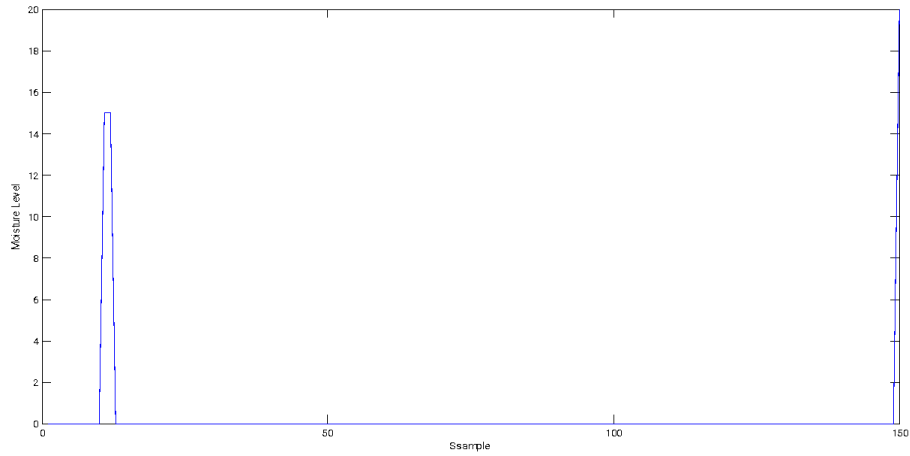
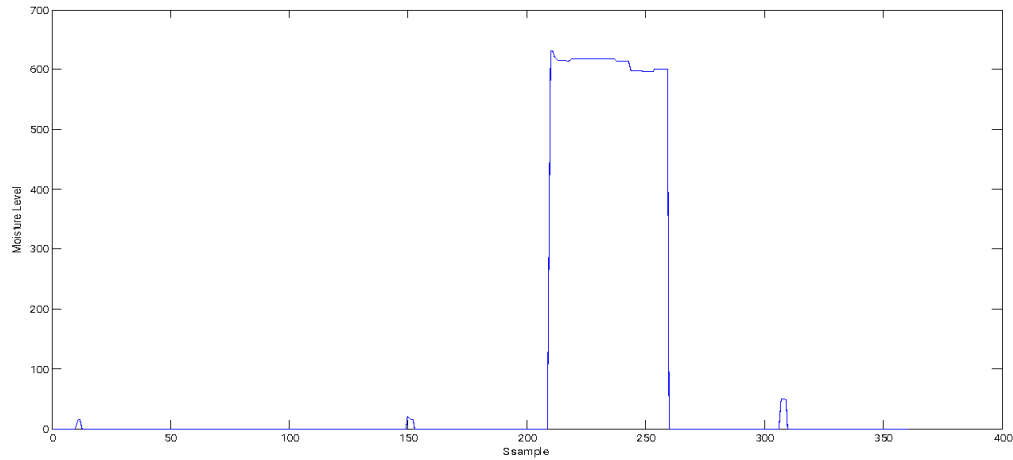


Figure 23

Moisture data – second window.



For moisture change event detection, a real-time experimental setup has been installed, data is acquired and Pearson coefficient of correlation between two successive data windows is computed. Figures 22 and 23 show the measured moisture levels and the resulting coefficient is -0.01. Which indicates a major change is soil drought. To test the Statistical Significance of correlation coefficient: the T-test is found to be -1.2243. To test the hypothesis that there is no linear association among the variables in the case of sudden change in moisture sensor data.

$$\begin{aligned}
 H_0: \rho &= 0. \\
 H_1: \rho &\neq 0. \\
 \alpha &= 0.05.
 \end{aligned}
 \tag{14}.$$

Which supports the decision: Accept the hypothesis of no linear association which indicated No drought as a new event.

6.1.4 Moment of Inertia Based Novelty Detection

The moment of inertia for N discrete point masses m_i distributed about a fixed y-axis, is [22]:

$$I_{y=} = \sum_{i=1}^N m_i x_i^2
 \tag{15)}.$$

Where x_i is the distance between the point mass m_i and the y-axis. In this paper the sensor reading is considered as a point mass. The y-axis is considered as the axis passing through $x=0$. Experiments have been performed in real time. Table 3. Shows the moment of inertia for three normal cases and three abnormal cases with sudden

illumination change. Sensor reading are normalized before calculating the moment of inertia.

Case Study: Light Change Event Detection

Table 3

Moment of Inertia for Event Detection

Case	1	2	3
Normal light	-00.5030	-01.7052	-00.1667
Suddenly changed light	-22.6945	-16.9603	-23.7065

6.1.5 Minimum ratio [18, 23]:

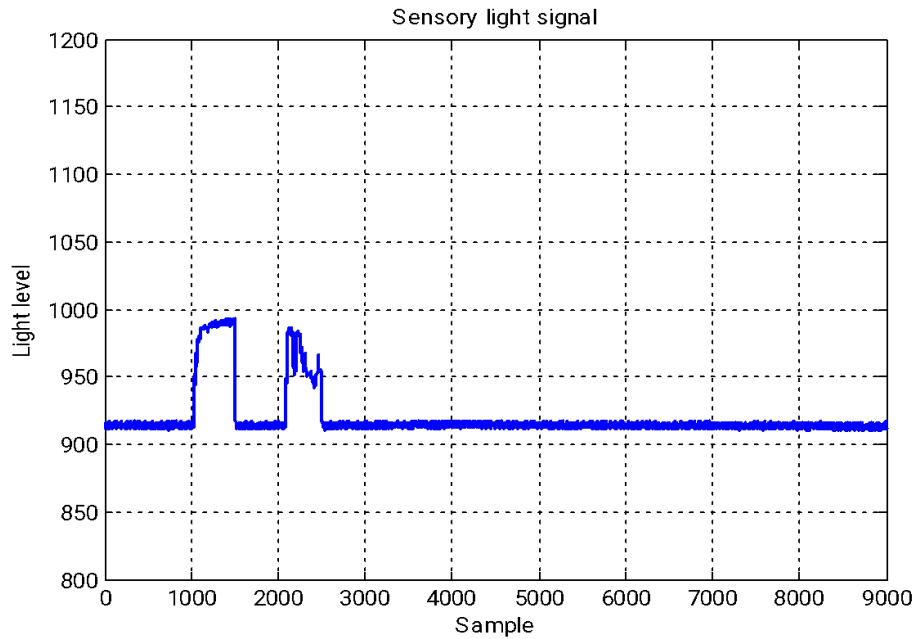
The minimum ratio (MR) is one of the well-known distance measures and is given by the following formula:

$$m_r = \frac{1}{n} \sum_i \min \left\{ \frac{h_i}{g_i}, \frac{g_i}{h_i} \right\} \quad (16)$$

It has been applied in this paper as a measure of distance between successive real-time data windows as a tool for novelty detection in sensor signals. Figure 23 shows a real time signal and the minimum ration between each two successive windows with each having 500 samples. It is clear from Figure 24 that the noisy sensor signal windows result in an MR value of approximately one. Changes in light levels (novelties in signal behavior) result is lowering the value of MR. A training set is used to identify the threshold limit below which abnormal events could happen.

Figure 24

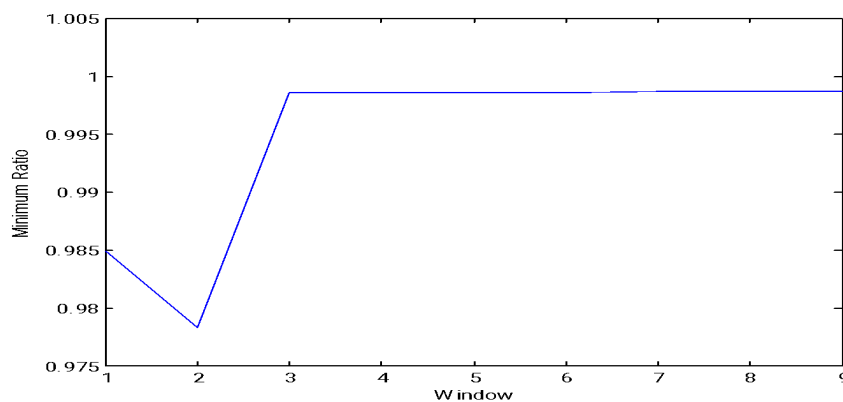
Light Signal with Abnormal Event.



The minimum ratio of successive signal windows resulted in excellent novelty detection performance as could be noticed from Figure 25. The MR decreases in case of sudden light change (Figure 24). The MR values for 9 successive windows taken from 9000 acquired samples are: 0.9848 0.9783 0.9985 0.9986 0.9986 0.9986 0.9986 0.9986 0.9986. The first two values correspond to the sudden changes in the first 500 samples.

Figure 25

Minimum ratio between successive windows.



6.1.6 Coefficient of Variation (COV)

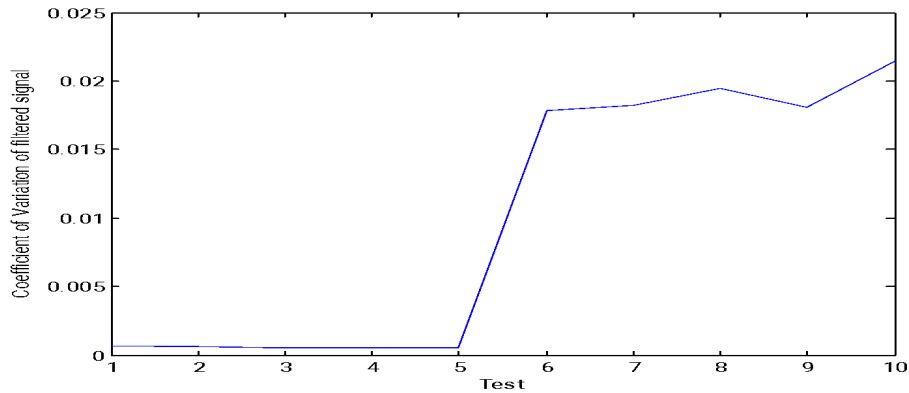
The coefficient of variation of 1D signal values is a measure of dispersion and is used here as a measure for novelty detection. COV is defined by:

$$COV = \frac{\sigma}{\mu} \times 100 \quad (17).$$

Where σ is the standard deviation and μ is the mean value. Figure 26 the change of the coefficient of variation with the occurrence of novel event in the sensor signal. Five light signals were acquired under normal light state and 5 signals were acquired under sudden light change conditions. The high discriminative power of the COV is very clear from Figure 26.

Figure 26

Coefficient of variation for 5 normal- and 5 abnormal cases.



(1) Novelty detection in sensor signals using Probabilistic Neural Networks

To avoid change in the environmental conditions which imply change of the threshold level which is used for novelty detection, the Probabilistic Neural Network (PNN) [19, 24] is training for novelty detection. PNN is training on 50 normal cases and 50 cases with events. The accuracy of PNN is 98%.

(2) Computational Complexity

For N_s samples of the sensor signal, and N_L lags of the auto-correlation function, the computational complexity is $O(N_s \times N_L)$. Therefore, the number of samples and lags directly influences the computational complexity. If calculated in the Frequency domain using FFT, the computational complexity is reduced to $O(N_s/2 \log_2 N_s)$. The computational complexity of minimum ration is on the order of N_s .

7. Conclusions and Future Work

Optimal sensor placement in smart homes aims at complete coverage, cost reduction and minimization of energy consumption. A heuristic strategy is presented for sensor placement through cooperation of multiple sensors. Wireless cams, passive infrared sensors (PIRs) and RFIDs cooperate through a master gateway. New algorithms are presented for the cooperative control of the smart home environment to guarantee complete coverage of the important areas in a smart home in such a way to monitor the activities of inhabitants and ensure the reliability of the system. System performance is evaluated through an intensive use in a real home setting. Experiments have been conducted for real scenarios in a smart home. Results indicated complete coverage of home areas, optimal number of sensors and high savings in both energy consumption and video-storage requirements. The statistical significance of important event detection features has been proven.

References

1. State of the Smart Home, Icontrol State of the Smart Home 2015, “https://www.icontrol.com/wp-content/uploads/2015/06/Smart_Home_Report_2015.pdf”, Last visited 22-10-2016 .
2. L. Kurkinen, “Smart Homes and Home Automation”, M2M Research Series, Berg Insight, 2016.
3. J. Lifton , M. Feldmeier , Y. Ono , C. Lewis , J. A. Paradiso , “A platform for ubiquitous sensor deployment in occupational and domestic environments”, international conference on information processing in sensor networks, IPSN '07. ACM, New York, pp 119–127. doi:10.1145/1236360.1236377], 2017.
4. L. Brian, S. A. ThomasEmail, J. C. CrandallDiane, “A Genetic Algorithm approach to motion sensor placement in smart environments”, Journal of Reliable Intelligent Environments, Volume 2, Issue 1, pp 3–16, April 2016.
5. J. Ranieri, A. Chebira , M. Vetterli, “Near-optimal sensor placement for linear inverse problems”, IEEE Trans Signal Process, 62(5):1135–1146. doi:10.1109/TSP.2014.2299518, 2014.
6. C. E. Rasmussen, “Gaussian processes in machine learning” , Advanced lectures on machine learning, Lecture notes in computer science, vol 3176, Springer, Berlin, pp 63–71. doi:10.1007/978-3-540-28650-9_4], 2004.
7. C. Guestrin ,A. Krause ,A. P. Singh, “ Near-optimal sensor placements in gaussian processes”, Proceedings of the 22nd international conference on machine learning, ICML '05. ACM, New York, pp 265–272. doi:10.1145/1102351.1102385, 2005 .
8. A. Krause, C. Guestrin , A. Gupta , J. Kleinberg , “Near-optimal sensor placements: maximizing information while minimizing communication cost”, Proceedings of the 5th international conference on information processing in sensor networks, IPSN '06. ACM, New York, pp 2–10. doi:10.1145/1127777.1127782. 2006.
9. M. Fantì, M. Roccotelli, J. Lesage, G. Faraut. “Motion Detector Placement Optimization in Smart Homes for Inhabitant Location Tracking”, ETFA'16: 21st IEEE Int. Conf. on Emerging Technologies and Factory Automation, Berlin, Germany. Sep 2016.
10. S. Khan, M. Shah, “Consistent labeling of tracked objects in multiple cameras with overlapping fields of view”, IEEE Transactions on Pattern Analysis and Machine Intelligence, vol. 25, no. 10, pp. 1355–1360, 2003.

11. X. Zhou, R. T. Collins, T. Kanade, P. Metes, "Amasterslave system to acquire biometric imagery of humans at distance", Proceedings of the 1st ACM SIGMM International Workshop on Video Surveillance, pp. 113–120, New York, NY, USA, 2003.
12. L. P. Kaelbling, M. L. Littman, and A. R. Cassandra, "Planning and acting in partially observable stochastic domains" , Artificial Intelligence, vol. 101, no. 1-2, pp. 99–134, 1998.
13. H. Zhang, H. C. Yan, F. W. Yang, and Q. J. Chen, "Quantized control design for impulsive fuzzy networked systems", IEEE Transactions on Fuzzy Systems, vol. 19, no. 6, pp. 1153–1162, 2011.
14. A. Hampapur, S. Pankanti, A. Senior, Y. L. Tian, L. Brown, R. Bolle, "Face cataloger: multi-scale imaging for relating identity to location", Proceedings of the IEEE Conference on Advanced Video and Signal Based Surveillance, pp. 13–21, Washington, DC, USA, 2003.
15. M. Ostland, H. Paula, S. Russell, and Y. Ritov, "Tracking many objects with many sensors", Proceedings of the International Joint Conferences on Artificial Intelligence (IJCAI '99), Stockholm, Sweden, 1999.
16. E. Essa, M. S. Hossain, A. S. Tolba, H. M. Raafat, S. Elmogy, and G. Muahmmad, "Toward cognitive support for automated defect detection," Neural Computing and Applications, vol. 32, pp. 4325–4333, 2019..
17. K. Mohammeda, A. S. Tolba, and M. Elmogy, "Multimodal student attendance management system (MSAMS)," Ain Shams Engineering Journal, vol. 9, pp. 2917–2929, 2018.
18. H. M. Raafat, M. S. Hossain, E. Essa, S. Elmougy, A. S. Tolba, G. Muhammad, A. Ghoneim, "Fog Intelligence for Real-time IoT Sensor Data Analytics", IEEE Access, vol. 5, pp. 24062-24069 , Sep 2018.
19. Gas Sensor, Research Design Lab, "<https://researchdesignlab.com/>", Last accessed July 2016 .
20. M. T. Abduridha, A. S. Tolba and M. Z. Rashad, "Complete Ensemble Empirical Mode Decomposition (CEEMD) for Real-Time Signal Detrending", IOT Applications International Journal of Intelligent computing and Information Sciences Ainshams Uni, 2016.
21. H. A. Khalaf , A. S. Tolba , M. Z. Rashid, "Event Triggered Intelligent Video Recording System Using MS-SSIM for Smart Home Security", Ain Shams Engineering Journal, October, 2016.
22. B. M. Dan," Mechanical Engineer's Handbook", Page 118, 2001.
23. A. A. Goshtasby, "Image Registration, Advances in Computer Vision and Pattern Recognition" , © Springer-Verlag London Limited, Chapter 2 Similarity and Dissimilarity Measures, DOI 10.1007/978-1-4471-2458-0_2, 2012.
24. F. D. Specht, "Probabilistic Neural Networks", Neural Networks, Vol. 3. pp. 109 118, 1990.